VERIFICATION

# UDM CHAPTER 4: HEAVY GAS DISPERSION

DATE: December 2023



| No. | Date | Reason for Issue | Prepared by | Verified by | Approved by |
|---|---|---|---|---|---|
| 1 | 1999 | PHAST 6.0 | Witlox and Holt | | |
| 2 | May 2011 | Phast 6,7; UDM v2 | Harper | | |
| 3 | May 2021 | Apply new template | D. Vatier | | |

Date: December 2023

**Prepared by: Digital Solutions at DNV**

# ABSTRACT

The UDM theory and solution algorithm for steady-state ground-level heavy-gas dispersion has been investigated in detail:

1. The top-entrainment formulation (Richardson-number calculation and entrainment function) has been validated against the 2-D wind-tunnel experiments of McQuaid (steady-state ground-level dispersion of $CO_2$). Good agreement has been obtained. Moreover UDM results are shown to be in identical agreement against an analytical solution for a neutral ground-level jet (adopting the heavy-gas logic). After this change, the validation was redone and similar agreement against the experimental data was shown (without tuning to the experimental data).
2. A literature review is carried out for the crosswind gravity-spreading formulation. The new formulation has been validated against the isothermal HTAG wind-tunnel experiments. Future implementation of the collapse of gravity spreading is recommended.
3. For the HTAG experiments, the UDM has also been verified against results of the HGSYSTEM model HEGADAS.
4. In the future, a further sensitivity analysis is recommended to be carried out for a given base-case problem, with a selected number of single/multiple parameter variations.

# Table of contents

# 4 HEAVY-GAS DISPERSION

## 4.1 Introduction

This report documents the verification and sensitivity analysis of the Unified Dispersion Model (UDM) for the case of continuous isothermal ground-level heavy-gas dispersion.

The literature regarding validation on heavy-gas dispersion has first been reviewed. An overview of heavy-gas-dispersion formulations is given both in the CCPS guidelines for vapour dispersion[i] and documentation by Lees[ii]. Also reference is made to the formulation in the HGSYSTEM heavy-gas dispersion program HEGADAS; see the HEGADAS theory manual[iii], the HGSYSTEM 1.0 Technical Reference manual[iv] , the HGSYSTEM 3.0 Technical Reference manual[v], and Witlox (1989)[vi].

During heavy-gas dispersion, the UDM applies the following entrainment equation and spreading equation,

$$\frac{dm_{cld}}{ds} = \frac{d}{ds}\left[2W_{eff}H_{eff}(1+h_d)u_{cld}\rho_{cld}\right] = \left[2W_{eff}u_{top} + H_{eff}(1+h_d)u_{side}\right]\rho_a + \frac{dm_{wv}^{\ gnd}}{ds}, \quad u_{side} = \gamma\frac{dW_{eff}}{dt}, u_{top} = \frac{\kappa\, u_*}{\Phi(Ri_*)}$$

$$\frac{dW_{eff}}{dt} = C_E\, u_*\, \sqrt{Ri_*}$$

Here $u_{top}$ is the top-entrainment velocity, $u_{side}$ the side-entrainment velocity, and $Ri_*$ the Richardson number; see the UDM theory manual for further details.

In Section 4.2 the evaluation of the Richardson number $Ri_*$ and the top-entrainment formulation (formula for $u_{top}$) is investigated, and compared with the literature.

In Section 4.3 the UDM equations are given for isothermal continuous ground-level heavy-gas dispersion. From this a reduced set of simplified equations is derived for the case of zero cross-wind spreading (2D dispersion; top-hat profile). These equations can be solved analytically in the case where an averaged, constant Richardson number is assumed.

In Section 4.4 the UDM is validated against the two-dimensional McQuaid experiments involving isothermal ground-level heavy-gas dispersion of carbon dioxide over flat terrain (2D dispersion without cross-wind spreading).

In Section 4.5 the UDM side-entrainment and cross-wind spreading formulation is investigated, and compared with the literature. In Section 4.6 the new formulation is validated against the HTAG experiments, involving isothermal ground-level heavy-gas dispersion over flat terrain (3D dispersion including cross-wind spreading).

Section 4.7 discusses possible further work.

## 4.2 Top-entrainment

### 4.2.1 Overview of formulations

As described above, the top-entrainment formulation is expressed by the top-entrainment velocity $u_{top}$ in terms of the entrainment function $\Phi(Ri_*)$, which is a function of the Richardson number $Ri_*$. The top-entrainment formulations have been compared for a range of commonly used similarity heavy-gas-dispersion models:

- the old and new UDM models (UDM5.2, UDM 6.7)
- the HGSYSTEM model HEGADAS[iii,v]
- the model DEGADIS[vii], which formulation is largely based on HEGADAS
- a formulation applied by Witlox (1989)[vi] in a 2D test version of the HEGADAS formulation, partly based on entrainment function proposed by Britter (1988)[viii]
- the HGSYSTEM model AEROPLUME[v]

Table 1 summarises the top-entrainment formulations for these models.

**Table 1. Top-entrainment formulations**

| MODEL | $Ri_*$ | $u_{top}$ | $\Phi(Ri_*)$ [$\Phi(0)=1$] |
|---|---|---|---|
| **UDM 5.2** | $g \min[\frac{\rho_{cld}-\rho_a(z_c)}{\rho_{cld}},5] H_{eff}(1+h_d)$ | $\alpha\, k_3\, u_*/\Phi(Ri_*)$<br>$\alpha\, k_3$ =.54 (A),.34 (D), .24(F) | $(1+0.8Ri_*)^{0.5}$, $Ri_*>0$<br>1, $Ri_*<0$ before lift-off<br>max{.003,$(1+0.65\|Ri_*\|^{0.6})^{-1}$}, $Ri_*<0$ after lift-off |
| **UDM 6.7** | $g\frac{\rho_{cld}-\rho_a(z_{cld})}{\rho_a(z_{cld})u_*^2} H_{eff}(1+h_d)$ | $0.4\, u_*/\Phi(Ri_*)$ | max{$Ri_*/7$ ,$(1+0.8Ri_*)^{0.5}/1.7$}, $Ri_*>2.3625$<br>1 , $0<Ri_*<2.3625$<br>$(1+0.65\|Ri_*\|^{0.6})^{-1}$, $Ri_*<0$ |
| **HEGADAS** | $g\frac{\rho_{cld}-\rho_a(H_{eff})}{\rho_a(z=0)u_T^2} H_{eff}$ | $0.41(1+p)\, u_T/\Phi(Ri_*)$ | $(1+0.8Ri_*)^{0.5}$, $Ri_*>0$<br>$(1-0.6Ri_*)^{-0.5}$, $Ri_*<0$ |
| **DEGADIS** | $g\frac{\rho_{cld}-\rho_a}{\rho_a u_*^2} H_{eff}$ | $0.4\, u_*/\Phi(Ri_*)$ | $1+0.11Ri_*^{1.04}$, $Ri_*>0$<br>$(1+0.65\|Ri_*\|^{0.6})^{-1}$, $Ri_*<0$ |
| **Witlox(1989) [Britter (1988)]** | $g\frac{\rho_{cld}-\rho_a}{\rho_a u_*^2} H_{eff}$ | $0.41\, u_*/\Phi(Ri_*)$ | $Ri_*/7$ , $Ri_* >14.72$<br>$(1+0.8Ri_*)^{0.5}/1.7$, $2.36<Ri_*<14.72$<br>1 , $0<Ri_*<2.36$ |
| **AEROPLUME** | $g\frac{\rho_{cld}-\rho_a}{\rho_a u_*^2}(2z_c)$ | $0.41\, u_*/\Phi(Ri_*)$ | max{$Ri_*/7$ ,$(1+0.8Ri_*)^{0.5}/1.7$}, $Ri_*>189/90$<br>1 , $0<Ri_*<189/90$<br>$(1-0.6Ri_*)^{-0.5}$, $Ri_*<0$ |

The following is noted.

1. Formula for effective cloud height

For a 2D (zero crosswind spreading problem), UDM, HEGADAS and DEGADIS adopt the same form of vertical concentration profile (exponent s) and wind-speed power-law profile (exponent p). As a result the formula for the effective height is the same for all these models.

$$H_{eff} = \Gamma(1+\frac{1}{n})R_z$$

2. Formula for Richardson number

The UDM 5.2 formula erroneously did not contain the friction velocity $u_*$. This has been corrected in the current UDM.

The UDM 5.2 adopts in the denominator of the formula for the Richardson number the term $\rho_{cld}$ while HEGADAS/DEGADIS adopt $\rho_a$. The latter assumption is also in line with the CCPS guidelines[i], and the method for which the entrainment correlations have been derived from experimental data. As a result the current UDM formula adopts $\rho_a$. For heavy gases the UDM 5.2 model results in a too small value of the Richardson number for high concentrations. For lower concentrations $\rho_a \approx \rho_{cld}$, and this difference will not have any effect.

HEGADAS modifies the friction velocity $u_*$ into $u_T$ if substrate heat transfer is taken into account. See Appendix C.3 of the HEGADAS theory manual. The extra term (1+p) appears to be a limitation of the HEGADAS passive-dispersion solution,

rather than a truly physical effect. This modification of the friction velocity may be considered for future implementation into the UDM.

3. Entrainment function, top-entrainment velocity

For $Ri_*>0$, the entrainment function formulation proposed by Britter (1988), and adopted by Witlox (1989) [and similar to McFarlane in AEROPLUME] are recommended since these lead to a best fit to available experiments data. As a result, this formulation is adopted in the current UDM. From Figure 4.1a it is seen that this formulation is also very close to the DEGADIS entrainment formulation. Note that for large Richardson numbers ($Ri_*>100$), the UDM 6.0/DEGADIS values for the top-entrainment are considerably less than for HEGADAS.

For $Ri_*<0$, the UDM adopts the entrainment function formulation adopted in DEGADIS. Figure 4.1b illustrates that the values for the entrainment function are in between the HEGADAS (p=0.1,0.7) values.

Note that unlike UDM 5.2, the new current UDM version does not include stability-class dependency of the top-entrainment velocity. For the far-field passive dispersion, the effect of stability class follows from the formula for the ambient vertical and cross-wind dispersion coefficients $\sigma_{za}$ and $\sigma_{ya}$. This implies reducing $\sigma_{za}$, $\sigma_{ya}$ and (increasing concentration, reduced entrainment) for increasing stability class.

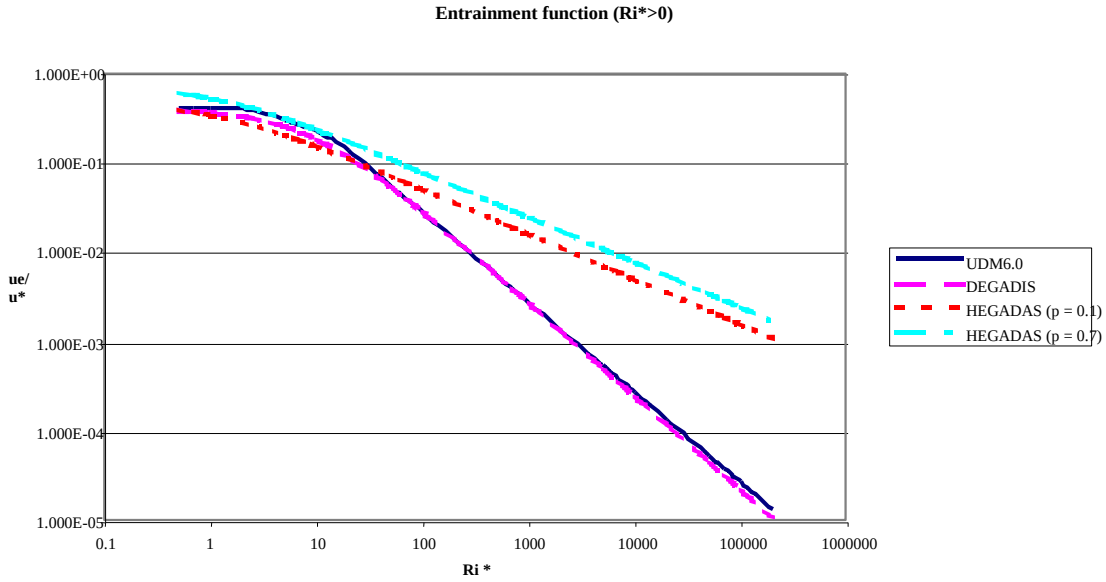


(a) Richardson number > 0

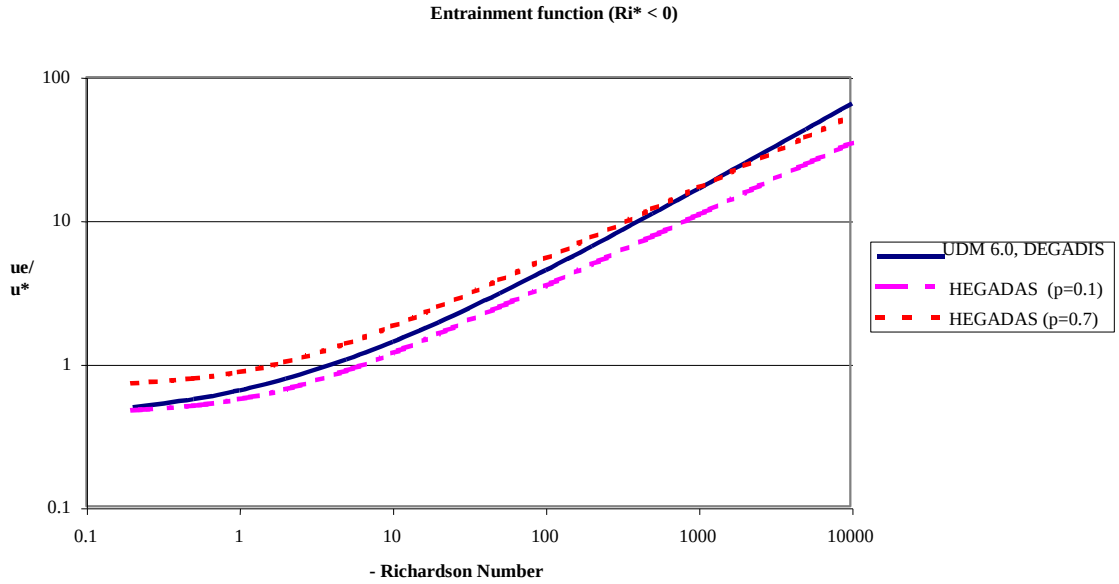


(b) Richardson number < 0

**Figure 4.1.** **Comparison of entrainment functions $\Phi(Ri_*)$ for UDM, DEGADIS and HEGADAS models; the plot displays the ratio of entrainment velocity to friction velocity [$u_{top}/u_* = \kappa / \Phi(Ri_*)$] as function of Richardson number $Ri_*$**

## 4.3 UDM equations

### 4.3.1 Isothermal continuous ground-level heavy-gas dispersion

The UDM theory manual includes a complete set of dispersion equations. For an isothermal, continuous, ground-level heavy-gas dispersion these equations simplify as follows:

- zero water-vapour transfer from ground: $m_{wvg}=0$

- no heat transfer from ground: $q_{gnd} = 0$
- zero vertical momentum: $I_z = 0$, $u_z = 0$, $z_{cld}$ = release height $z_R = 0$, $\theta=0$, $h_d = 0$
- zero horizontal excess momentum: $I_{x2} = 0$, $u_{cld} = u_a$ (cloud moving with the wind)
  [Note that for McQuaid experiments this is not valid for an area near the release point, at which the injection velocity differs from the ambient velocity; this will be ignored in the analytical solution which will may lead to some discrepancy between the analytical and numerical/experimental solutions near the source]
- enthalpy equation (isothermal, pure vapour, ideal gas): $T_{cld} = T_a$
  → density $\rho_{cld} = \rho_a [1 - c_{ov}] + \rho_{pol} [c_{ov}]$, with $c_{ov} = c_o/\rho_{pol}$
  [$c_{ov}$ = centre-line ground-level concentration (volume fraction = mole fraction),
  $c_o$ = centre-line ground-level concentration (kg of pollutant / $m^3$ of mixture)
  $\rho_{pol}$ = pollutant density at $T_a$ (kg of pollutant / $m^3$ of pollutant)
  $\rho_a$= air density at $T_a$ (kg of air / $m^3$ of air)]
  $\rho_{cld}$ = mixture density at $T_a$ (kg of mixture/ $m^3$ of mixture)]
- cloud area $A_{cld}(x) = 2 H_{eff}W_{eff}$
- cloud mass/area relation $m_{cld} = \rho_{cld}A_{cld}(x)u_a$
- pollutant conservation: mass-flow rate $c_oA_{cld}(x)u_a$ = constant = Q (kg of pollutant /s) or volume-flow rate $c_{ov}A_{cld}(x)u_a = Q / \rho_{pol}$ ($m^3$ of pollutant / s)
- air entrainment: $dm_{cld}/dx = Ent_{tot}$ (heavy and passive entrainment contributions)
  $dm_{cld}/dx = Ent_{heavy}$ = ….. (before passive transition)
  $dm_{cld}/dx = E_{pas} = A_{cld}(x)\, u_a\rho_a[\sigma_y^{-1}d\sigma_{ya}/dx+\sigma_z^{-1}d\sigma_{za}/dx]$ in far-field (transition in between)
- cross-wind spreading law: $dW_{eff}/dx$ = …..
- Richardson number: $Ri_* = [g (\rho_{cld}-\rho_a) / \rho_{cld}] H_{eff} / u_*^2$
- concentration-profile exponents: $m=m[(\rho_{cld} -\rho_a)/ \rho_a]$, $n= n[H_{eff}/L]$

After eliminating $A_{cld}(x)$, $M_{cld,}$ the following 7 equations remain for the 7 unknowns $\rho_{cld}$, $c_{ov}$, $H_{eff}$ [related to $\sigma_z$, $R_z$], $W_{eff}$ [related to $\sigma_y$, $R_y$], $Ri_*$, m,s

| | | |
|---|---|---|
| (a) | $\rho_{cld} = \rho_a [1 - c_{ov}] + \rho_{pol} [c_{ov}]$ | (density ) |
| (b) | $c_{ov} [2 H_{eff}W_{eff}u_a] = Q / \rho_{pol}$ | (pollutant conservation) |
| (c) | $d[2 H_{eff}W_{eff}\, u_a\rho_{cld}]/dx = Ent_{tot}$ = …. | (air entrainment) |
| (d) | $dW_{eff}/dx$ = ….. | (cross-wind spreading law) |
| (e) | $Ri_* = [g (\rho_{cld}-\rho_a) / \rho_{cld}] H_{eff} / u_*^2$ | (Richardson number) |
| (f) | $m=m[(\rho_{cld} -\rho_a)/ \rho_a]$ | (conc.profile exponent) |
| (g) | $n= n[H_{eff}/L]$ | (conc.profile exponent) |

## 4.3.2 Simplified equations for no cross-wind spreading; analytical solution

For neutral stability L=∞ and therefore n=2. For uniform cross-wind profile m=∞ and 2 $W_{eff}$ = 2 $R_y$ = constant = (take) 1. Moreover Q = release rate (kg of pollutant /m of cross-wind direction /s). Assuming heavy-gas entrainment only (no passive transition), this leads to the following further reduced 3 equations for $\rho_{cld}$, $c_{ov,}$ $H_{eff}$ [=$\Gamma(3/2)R_z = 0.5\pi^{1/2}$ $R_z = 0.5(2\pi)^{1/2}$ $\sigma_z$].

| | | |
|---|---|---|
| (a) | $\rho_{cld} = \rho_a [1 - c_{ov}] + \rho_{pol} [c_{ov}]$ | (density) |
| (b) | $c_{ov} [H_{eff}u_a] = H_{release}u_{release} = Q / \rho_{pol}$ | (pollutant conservation) |
| (c) | $d[H_{eff}u_a\rho_{cld}]/dx =\rho_a u_{top} = \rho_a\ \kappa\, u_* / \Phi(Ri_*)$, $Ri_*=[g (\rho_{cld}-\rho_a)/ \rho_a]H_{eff}/u_*^2$ | (air entrainment) |

Eliminating $\rho_{cld}$, $c_{ov}$ using the first two equations, this leads to a differential equation for $H_{eff}$ that can easily be solved in the downwind direction using the starting condition $H_{eff}(x=0) = H_{release}$. Note that $u_a$ varies as function of z, while $\rho_a$ can be taken to be constant

## 4.3.3 Analytical solution assuming constant Richardson number

For the Richardson number $Ri_*$ assumed to be constant = $Ri_*0$, the differential equation can be solved analytically

$$H_{eff}\, u_a\rho_{cld} = [\alpha k_3 u_*/\Phi(Ri_{*0})]\, x + (\rho_{cld}\, H_{eff}u_a)_{release} = [\alpha k_3 u_*/\Phi(Ri_{*0})]\, x + Q$$

Therefore

$$c_{ov} = \frac{1}{1 + \left(\frac{\kappa u_* \rho_{pol}}{Q\,\Phi(Ri_*)}\right) x}$$

The following is noted.

1. The above solution should correspond exactly to the numerical solution, if in the numerical solution $Ri_* = Ri_{*0}$ would be adopted and the pollutant would have been released with exactly the ambient velocity. Since the latter does not occur, some discrepancy will occur.

2. Alternatively the numerical solution could be started at a downwind distance at which the velocity is reduced to the ambient velocity. Downwind of this distance the above analytical solution can be applied. In that case it can be shown that the above solution comes down to the exact same solution as the HEGADAS solution for $c_{ov}$ by Witlox (1989).

3. Note that if $Ri_* < 2.35$ and wind speed reduce to ambient speed, the analytical solution would also be exact.

   The pollutant mass flow can be shown to be given by [analogous to Witlox (1989)]

$$Q = \int_0^\infty c\,u\,dz = \int_0^\infty c_0 e^{-(z/R_z)^n} u_{ref}\left(\frac{z}{z_{ref}}\right)^p dz = \frac{1}{n} c_0 u_{ref} z_{ref} \Gamma\left(\frac{1+p}{n}\right)\left(\frac{R_z}{z_{ref}}\right)^{1+p} = c_0 u_a(z=R_z)\frac{1}{n}\Gamma\left(\frac{1+p}{n}\right)R_z \quad \textbf{(1)}$$

   Note that the above equation is different to the UDM equation for imposing mass conservation

$$Q = c_o u_a(z=z_c)\, H_{eff} = c_o u_a(z=z_c)\,\Gamma(1+1/n) R_z\,,\quad z_c = \frac{R_z}{2}\frac{\Gamma\left(1+\frac{2}{n}\right)}{\Gamma\left(1+\frac{1}{n}\right)} \qquad \textbf{(2)}$$

   The above expressions ( 1 )and ( 2 ) are identical in case of an uniform wind speed (p=0). However, for a non-uniform wind speed UDM mass may not be exactly conserved, and as a result the values for $R_z$ are different (although for small values of p the effect will be small). The resulting difference in the values for $R_z$ will be investigated using the McQuaid experiments.

4. Further data can be derived as follows from the above data

   - $c_o = \rho_{pol}\, c_{ov}$
   - $A_{cld}(x) = 2\, H_{eff} W_{eff} = H_{eff}$
   - $\rho_{cld} = \rho_a\,[1 - c_{ov}] + \rho_{pol}\,[c_{ov}]$
   - $m_{cld} = \rho_{cld} A_{cld}(x) u_a$

## 4.4 Validation against 2D McQuaid experiments

In the previous section simplified UDM equations have been derived for steady-state 2D isothermal ground-level heavy-gas dispersion, and an analytical solution has been given assuming a constant Richardson number. In this section the numerical solution of these equations by the UDM will be validated against experiments carried out by McQuaid[ix]. Note that previous simulations against the McQuaid experiments were carried out for a 2D test version of HEGASAS, the finite-element programs FEM3 and FEMSET, and the finite-volume code FLOW3D; see Witlox[vi,x] for further details.

### 4.4.1 Experimental parameters and results

A set of three wind-tunnel experiments were carried out by McQuaid. The experiments are characterised by the following:

- steady-state release of carbon dioxide ($CO_2$) by a line source of width $L_p$ = 0.05 m and injection velocity $v_l$ given in Table 2. Thus the release rate equals $Q = \rho_{pol} v_l L_p$ (kg/m/s)
- dispersion over flat terrain
- isothermal flow (temperature = 293.5K)
- a logarithmic formula for the ambient wind speed $u_a(z) = (u_*/\kappa)\ \ln(1+z/z_R^*)$, with the friction velocity $u_*$ and the equivalent surface roughness $z_R^*$ given in Table 2 and $\kappa$ the Von Karman constant (UDM assumes $\kappa$=0.40, while McQuaid assumed $\kappa$=0.41)

McQuaid postulated for the concentration $c_v$ (mole or volume fraction)

$$c_v(x,z) = c_{ov}(x)\exp\left[-\ln(2)\left(\frac{z}{H_{1/2}}\right)^n\right]$$

where $c_{ov}(x)$ is the ground-level concentration, and $H_{1/2}(x)$ the height at which $c_v$ is halved.
The measured data for $c_{ov}(x)$ and $H_{1/2}(x)$ were found to be accurately fitted by power-laws for 0.5 m< x < 5 m. McQuaid recommends n = 2.14, while Britter[viii] advises n = 1.5.

**Table 2.** Experimental data by McQuaid: values of parameters [release rate Q, friction velocity $u_*$, injection velocity $v_l$, equivalent surface roughness $z_R$*, wind speed $u_a(0.1)$ at height 0.1 m, wind-speed power-law exponent p] and measurements [power-laws for ground-level concentration $c_{ov}$ and height $H_{1/2}$ at which concentration is halved(from fit to experimental data, valid for 0.5 m < x < 5 m)]

| Exp. | Q (kg/m/s) | $u_*$ (m/s) | $v_l$ (m/s) | $z_R^*$ (m) | $u_a(0.1)$ | p | $c_{ov}(x)$ (mole fr.) | $H_{1/2}(x)$ (m) |
|---|---|---|---|---|---|---|---|---|
| **1** | 0.0113 | 0.144 | 0.123 | $1.37*10^{-5}$ | 3.12 | 0.132 | $0.082*x^{-0.88}$ | $0.043*x^{0.54}$ |
| **2** | 0.0142 | 0.073 | 0.155 | $2.59*10^{-5}$ | 1.47 | 0.144 | $0.190*x^{-0.84}$ | $0.037*x^{0.55}$ |
| **3** | 0.0226 | 0.053 | 0.247 | $3.60*10^{-5}$ | 1.03 | 0.151 | $0.395*x^{-0.36}$ | $0.046*x^{0.17}$ |

### 4.4.2 UDM predictions

<u>UDM simulation</u>

UDM simulations for the above problem were carried out as follows.

1. The UDM power-law fit of the logarithmic profile is appropriate for atmospheric conditions, and does not lead to accurate results for the smaller wind-tunnel dimensions. As a result the power-law exponent p was imposed. For experiment 2 the power-law exponent p was obtained from Witlox [iii]. For experiments 1,3 it was obtained by using the more advanced power-law fit algorithm in HEGADAS. The applied input data are given in Table 2.

2. The 2D conditions (with no cross-wind spreading) were imposed as follows:

   - The cross-wind concentration exponent m = $\infty$ is imposed (the large value m = 50 is adopted), to apply a top-hat profile with no cross-wind concentration variations.
   - The equation $dR_y/ds = 0$ is imposed to apply zero gravity spreading. This is done by setting the cross-wind gravity spreading parameter $C_E$ = 0.

   The above implies that the 'cloud width' = $2\,W_{eff} = 2R_y$ is a constant, which is chosen to be $W_{eff}$ = 1.

3. The source is modelled as a vertical source at x = 0, with a horizontal release velocity $v_l$ (m/s) and flow rate Q (kg/m/s)[1].

4. Isothermal flow ($T_a$ = 293.5 K, $P_a$ = 1 atm.) is assumed with uniform pressure/temperature profiles, and a power-law wind speed profile with cut-off at 0.01 m.

5. The default value n=2 is used for the vertical concentration exponent n. This value matches closely the recommended value n = 2.14 by McQuaid, although Britter[viii] advises n = 1.5.

UDM results

First a UDM simulation was carried out for experiment 2, in which a constant Richardson number $Ri_* = 5.7$ was hardwired. This value was found by McQuaid to be the 'average Richardson number'. Figure 4.2 demonstrates that the UDM results are in almost exact agreement with the results obtained from the analytical solution derived in Section 4.3.3. Note that also data for other variables were found to be almost identical. Thus this verifies the correct implementation of the heavy-gas top-entrainment formulation.

Equation ( 1 ) contains an analytical expression for mass conservation assuming the cloud speed to be equal to the ambient wind-speed. Equation ( 2 ) is the mass-conservation equation adopted by the UDM. Figure 4.3 compares the analytical pollutant mass flow rate ( 1 ) with the actual value of the flow rate Q = 0.0226 (kg/m/s) for experiment 3 of McQuaid. The reason of the discrepancy is the fact that Equation ( 1 ) assumes the ambient wind-speed for the cloud speed, which is too high near the source. Thus this equation provides a too high estimate for the source rate Q near the source. Further away from the source the cloud speed speeds up to the ambient speed and Equation ( 1 ) becomes valid. Note that the significant differences between cloud and ambient speed near the source also imply that jet entrainment needs to be taken into account.

Secondly UDM simulations have been carried out including the calculation of the Richardson number. Figure 4.4, Figure 4.5, Figure 4.6 include UDM predictions for McQuaid experiments 1, 2, 3, respectively. These figures include three type of UDM simulations:

1. The first run assumes the total entrainment $E_{tot}$ to consist of heavy-gas entrainment $E_{hvy}$ only: $E_{tot} = E_{hvy}$. This results in an over-prediction of the ground-level concentration and an under-prediction of the height $H_{1/2}$. This seems to be caused by the neglect of the jet entrainment $E_{jet}$.

2. The second run adopts the UDM 5.2 assumption for the total entrainment to be the sum of jet and heavy-gas entrainment: $E_{tot} = E_{hvy} + E_{jet}$. This results in considerably improved predictions for all three experiments.

3. McFarlane[v] observes that jet-entrainment and heavy-gas entrainment are not independent mechanisms. In line with this the third run adopts the current UDM assumption of the total entrainment to be the maximum of jet and heavy-gas entrainment: $E_{tot} = \max(E_{hvy}, E_{pas})$. This is seen to further improve the predictions for experiment 3, but to reduce somewhat the accuracy for experiment 2.

[1] Note that for the actual experiment, the source was a ground-level source with a vertical velocity $v_l$. It is however expected that this will not significantly affect the results. This should need preferably further investigation.

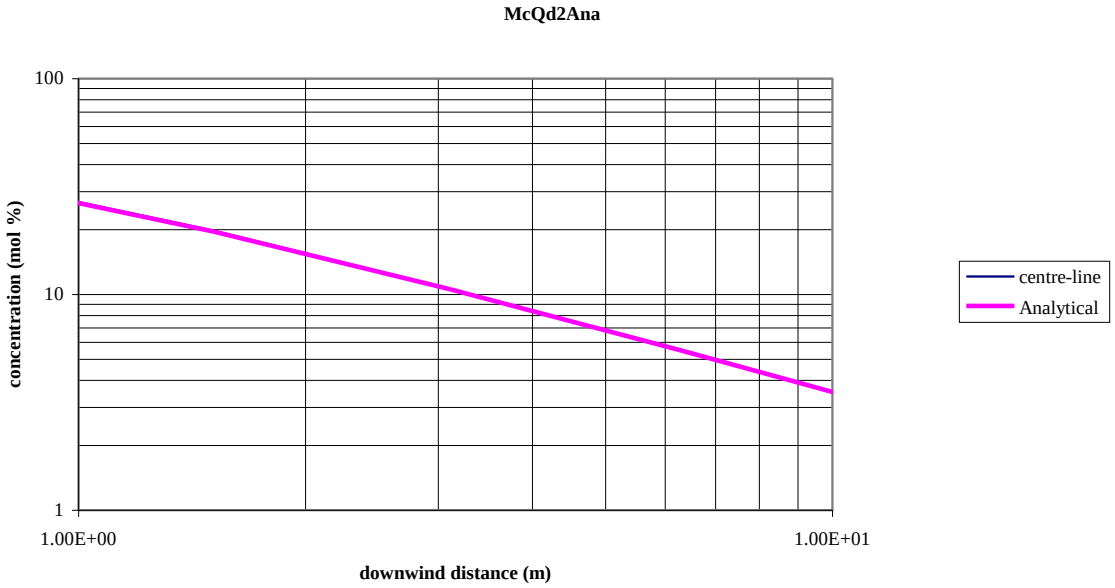


**Figure 4.2.** **Comparison of the UDM predictions for experiment 2 of McQuaid, in which the Richardson number has been hardwired to a value of 5.7, with the analytical solution.**

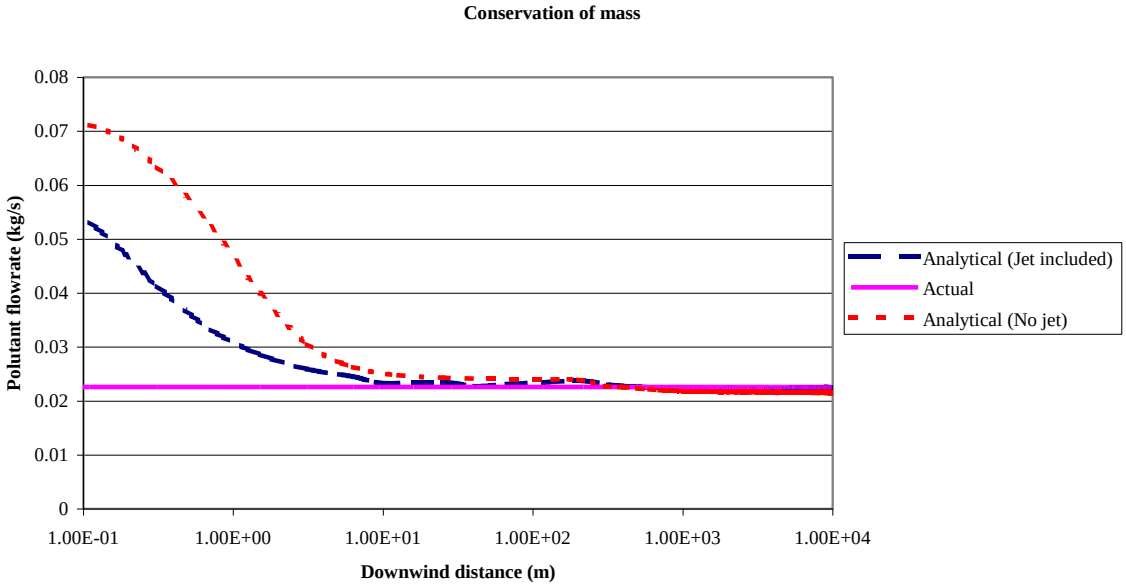


**Figure 4.3.** **Comparison of the analytical pollutant mass flow rate with the actual value for experiment 3 of McQuaid. The 'analytical' flow rates have been derived from Equation ( 1 ) for two types of UDM simulations ($E_{tot} = E_{hvy}$, and $E_{tot} = E_{hvy} + E_{jet}$).**

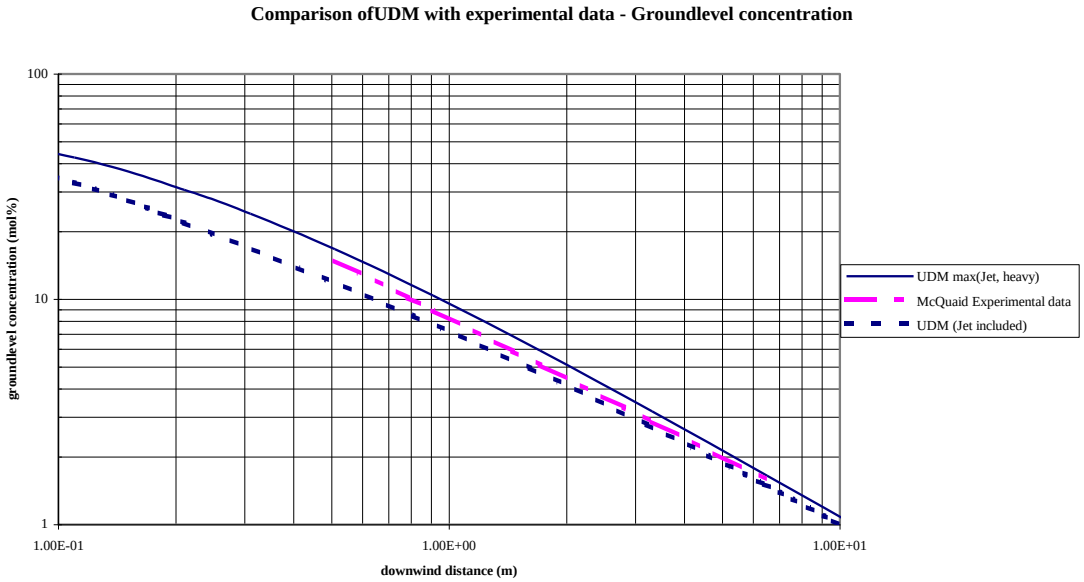


(a) ground-level concentration $c_{ov}$ (mole %)

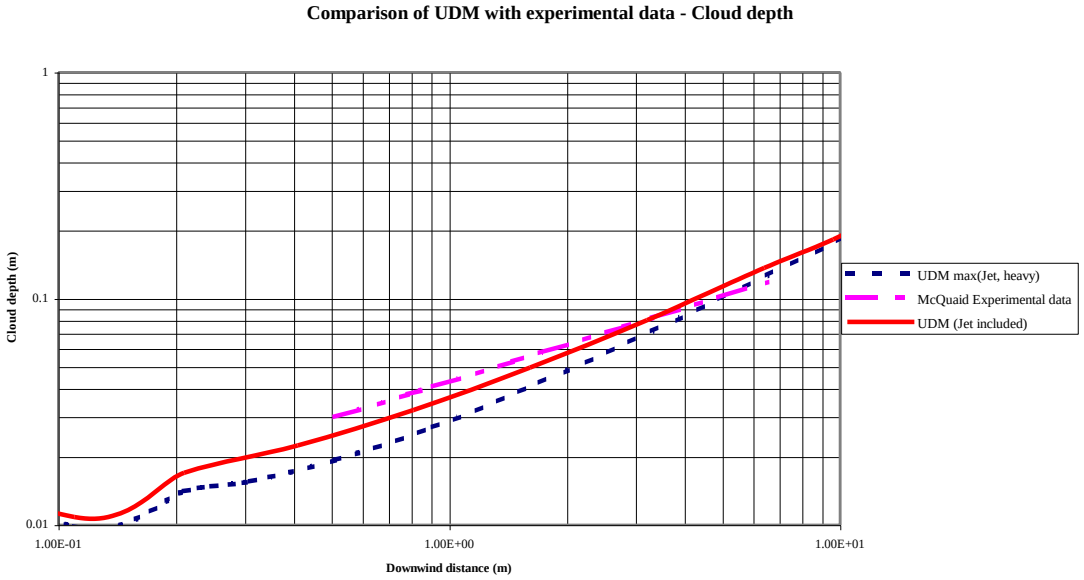


(b) height $H_{1/2}$ (m) at which concentration is halved

**Figure 4.4. McQuaid experiment 1; experimental data (fitted by straight line) and UDM predictions assuming (a) $E_{tot} = E_{hvy}$ [results not included] (b) $E_{tot} = \max(E_{hvy}, E_{jet})$, (c) $E_{tot} = E_{hvy} + E_{jet}$**

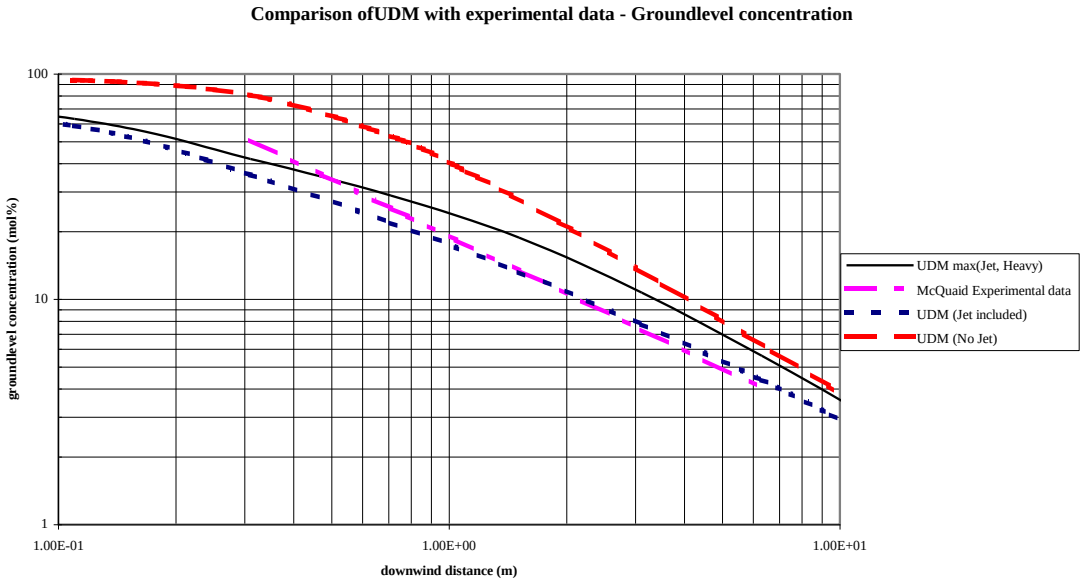


(a) ground-level concentration $c_{ov}$ (mole %)

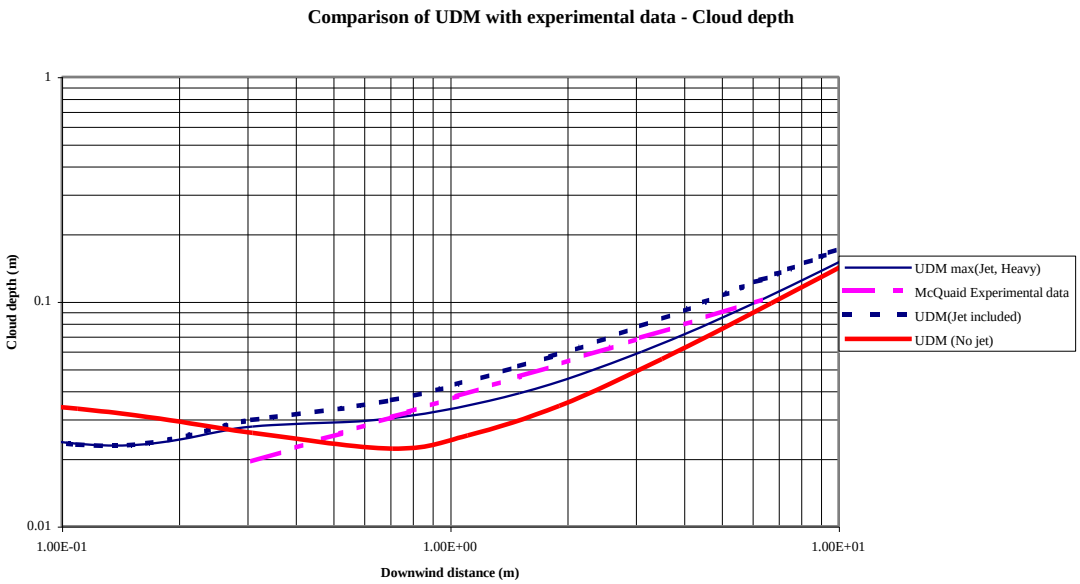


(b) height $H_{1/2}$ (m) at which concentration is halved

**Figure 4.5. McQuaid experiment 2; experimental data (fitted by straight line) and UDM predictions assuming (a) $E_{tot} = E_{hvy}$, (b) $E_{tot} = \max(E_{hvy},E_{jet})$, (c) $E_{tot} = E_{hvy}+E_{jet}$**

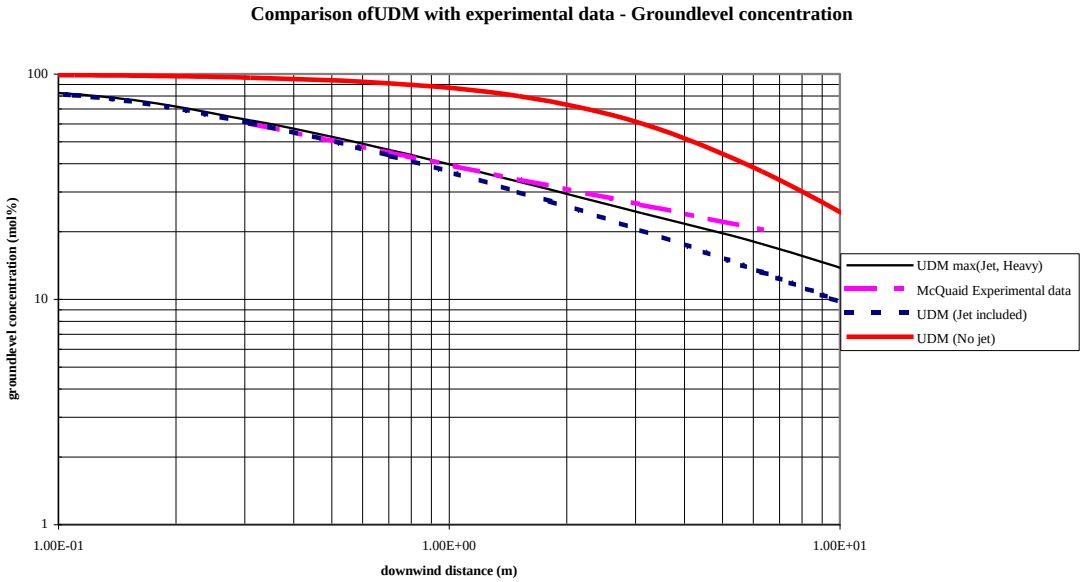


(a) ground-level concentration $c_{ov}$ (mole %)

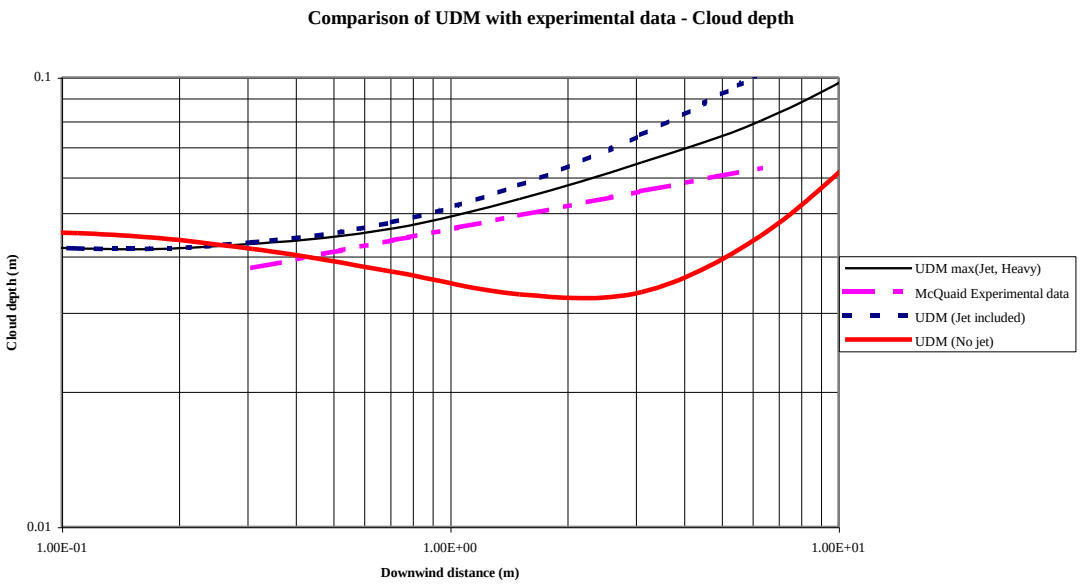


(b) height $H_{1/2}$ (m) at which concentration is halved

**Figure 4.6. McQuaid experiment 3; experimental data (fitted by straight line) and UDM predictions assuming (a) $E_{tot} = E_{hvy}$, (b) $E_{tot} = \max(E_{hvy},E_{jet})$, (c) $E_{tot} = E_{hvy}+E_{jet}$**

## 4.5 Cross-wind spreading and side entrainment

### 4.5.1 Overview of formulations

The table below includes an overview of crosswind-spreading and side-entrainment formulations.

**Table 3. Cross-wind spreading and side-entrainment formulations (continuous)**

| MODEL | spreading law | Ri | $C_E$ | $u_{side}$ |
|---|---|---|---|---|
| **SLAB** | ….. | ……. | ….. | $(1.8)^2(h/B)u_{top}$ |
| **DENZ** | ….. | ……. | ….. | $\gamma\, dW_{eff}/dt$<br>$\gamma = 0.$ |
| **UDM 5.2** | $dW_{eff}/dt = C_E u_* Ri^{0.5}$ | $g\frac{\rho_{cld}-\rho_a(z_c)}{\rho_{cld}}H_{eff}$ | $k_2^{0.5}$=.39 | $\gamma\, dW_{eff}/dt$<br>$\gamma = 0.05$ |
| **UDM (current)** | $dW_{eff}/dt = C_E u_* Ri^{0.5}$ | $g\frac{\rho_{cld}-\rho_a(z_c)}{\rho_{cld}u_*^2}H_{eff}$ | 1.15 | $\gamma\, dW_{eff}/dt$<br>$\gamma = 0$ |
| **HEGADAS** | $dW_{eff}/dt = C_E u_* Ri^{0.5}$<br>Reduced post-collapse spreading | $g\frac{\rho_{cld}-\rho_a(z=0)}{\rho_{cld}u_*^2}H_{eff}$ | 1.15 | 0 |
| **DEGADIS** | $dW_{eff}/dt = C_E u_* Ri^{0.5}$ | $g\frac{\rho_{cld}-\rho_a}{\rho_{cld}u_*^2}H_{eff}$ | 1.15 | 0 |
| **AEROPLUME** | dD/dt = …..<br>(to check)?? | $Ri_* = g\frac{\rho_{cld}-\rho_a}{\rho_a u_*^2}(2z_c)$ ?? | ??? | 0?? |

### 4.1.1 Gravity spreading formulation (current UDM)

In the UDM continuous model, the entrainment equation and the gravity-spreading equation are given by

$$\frac{dm_{cld}}{ds} = \frac{d}{ds}\left[2W_{eff}H_{eff}(1+h_d)u_{cld}\rho_{cld}\right] = \left[2W_{eff}u_{top} + H_{eff}(1+h_d)u_{side}\right]\rho_a + \frac{dm_{wv}^{\ gnd}}{ds}, \quad u_{side} = \gamma\frac{dW_{eff}}{dt}, u_{top} = \frac{\kappa\, u_*}{\Phi(Ri_*)}$$

$$\frac{dW_{eff}}{dt} = C_E\, u_*\sqrt{Ri_*}$$

where $m_{cld}$ is the cloud mass (kg/s) and $m_w$ the added water vapour from the substrate (kg/s).

The UDM 5.2 value of 0.39 for the gravity-spreading parameter $C_E$ is considerably smaller than the value of $C_E \approx 1.15$ adopted by most other models. The value for the gravity-spreading parameter $C_E$ is obtained in most dense-gas-dispersion models from experiments by Van Ulden[xi] for instantaneous gravity spreading ($C_E$ = 1.15; HEGADAS adopts $C_E$ = 1.15, while Britter uses in his workbook $C_E$ = 1.07; DENZ, CRUNCH apply similar values). As a result the current UDM default value is $C_E$ = 1.15.

Top entrainment is commonly assumed to be dominant to side entrainment for continuous heavy-gas dispersion. As a result in the current UDM, by default the side entrainment coefficient is selected to be $\gamma$=0. Note this resulted in a slight improvement of the predictions of the validation set of experiments.

The above equations are applied before the passive transition. Downwind of the passive transition the equations are as follows

$$\frac{dm_{cld}}{ds} = \frac{d}{ds}\left[2W_{eff}H_{eff}(1+h_d)u_{cld}\rho_{cld}\right] = 2W_{eff}\left[\frac{1}{\sigma_y}\frac{d\sigma_{ya}}{dx} + \frac{1}{\sigma_z}\frac{d\sigma_{za}}{dx}\right]u_a(z=z_c)\,\rho_a(z=z_c) + \frac{dm_{wv}^{\ gnd}}{ds}$$

$$\frac{d\sigma_y}{dx} = \frac{d\sigma_{ya}}{dx}$$

Note that passive dispersion is phased in along a transition zone.

## 4.5.2 Gravity-spreading formulation including collapse (HEGADAS)

The reduced value for $C_E$ as adopted in UDM 5.2 may result in better predictions in cases where the collapse of gravity spreading is significant (although the formulation does not represent the correct physics). The HGSYSTEM model HEGADAS includes gravity-spreading collapse. In the latest version 3.0 of HGSYSTEM the post gravity-spreading-collapse formulation has been modified with respect to that adopted in HGSYSTEM 1.0; see Chapter 7B in the HGSYSTEM 3.0 manual[v] and Roberts and Hall[xii]. This modification ensures a more smooth transition between the post gravity-spreading collapse criterion and the purely passive criterion. This formulation is summarised below.

The HEGADAS model[iii] adopts a similarity concentration profile, defined by

- a middle part with half-width b, along which the concentration is uniform
- outer Gaussian flanks with decay defined by the cross-wind dispersion coefficient $S_y = 2^{0.5}\sigma_y$

The effect cloud width is defined by $W_{eff} = b + 0.5\pi^{0.5}S_y$.

The HEGADAS model assumes that a dense gas cloud passes through three consecutive stages of lateral cloud growth:

1. *Gravity spreading*.

   The entrainment equation, gravity-spreading equation and the equation defining the growth of the Gaussian flanks are given by

$$\frac{1}{2W_{eff}}\frac{d}{dx}\left[\frac{2W_{eff}H_{eff}u_{eff}}{V_m}\right] = \frac{u_{top}(u_T)}{V_0} + Q_{wv}\ , \quad u_{top}(u_T) = \frac{\kappa\, u_T}{\Phi(Ri_*(u_T)}$$

$$\frac{dW_{eff}}{dt} = C_E\ u_*\ \sqrt{Ri}$$

$$S_y\frac{dS_y}{dx} = 2\left(\frac{2}{\pi}\right)^{0.5} W_{eff}\ \ \frac{d\sigma_{ya}}{dx}\left[x = \sigma_{ya}{}^{-1}\left(\left(\frac{2}{\pi}\right)^{0.5} W_{eff}\right)\right]$$

   In the entrainment equation the term between brackets represents the cloud molar flow through a vertical plane (kmole/s), $V_m$ is the mixture volume ($m^3$/kmole), $V_o$ = 22.4 $m^3$/kmole is the ideal-gas molar volume at 0C and 1 atmosphere, and $Q_{wv}$ the molar water-vapour flux from the surface. Note that HEGADAS adopts for the cloud speed the effective cloud speed, rather than the speed at the cloud centroid. In addition the entrainment equation is expressed in terms of cloud molar flow (kmole/s) rather than cloud mass flow (kg/s). Note that $\rho_{cld} = M_{cld}/V_m$, where $M_{cld}$ is the molecular weight of the cloud mixture.

   In the equation for $S_y$, $\sigma_{ya}{}^{-1}$ is the inverse function of the ambient passive dispersion coefficient $\sigma_{ya}(x)$.

   The above logic applies as long as the 'gravity current collapse criterion' is not satisfied, i.e.

$$\frac{u_{top}\,W_{eff}}{\dfrac{dW_{eff}}{dt}\,H_{eff}} = \frac{\kappa\,W_{eff}}{C_E Ri^{0.5}\Phi(Ri_T)H_{eff}} > \text{constant} = \frac{8(1+p)}{3C_E} = 2.32\,(1+p) \qquad \textbf{(3)}$$

   The values p=0.1, 0.7 lead to the values for the constant of 2.5 and 4.

   The term $W_{eff}\,u_{top}$ is the volumetric flow (per unit of length in the downwind distance) of air entrained at the top of the cloud, and the $H_{eff}$ ($dW_{eff}/dt$) is the added volume (per unit of time, and per unit of length in the downwind distance) due to lateral expansion. Thus when the ratio in the left-hand side of the above equation exceeds 1, the flow of air mixed into the top of the cloud exceeds the increase in cloud volume due to lateral expansion and the cloud height must increase, changing the vertical distribution of the dense gas. This process erodes the vertical density stratification within the body of the cloud that is needed to maintain the gravity current. Thus the above criterion is a measure of the destruction of the internal vertical structure of the gravity current by mixing driven by the external turbulence.

2. *Post-collapse gravity spreading (b>0).*

   After the above criterion is satisfied, the entrainment equation, gravity-spreading equation and the equation defining the growth of the Gaussian flanks are given by

$$\frac{d}{dx}\left[\frac{H_{eff}u_{eff}}{V_m}\right]=\frac{u_{top}(u_T)}{V_0}+Q_{wv}\ ,\quad u_e(u_T)=\frac{\kappa\, u_T}{\Phi(Ri_*(u_T)}$$

$$W_{eff}\ \frac{dW_{eff}}{dx}=\ 2^{-3/2}\,\pi\ S_y\ \ \frac{d\sigma_{ya}}{dx}\left[x=\sigma_{ya}{}^{-1}\left(2^{-0.5}\,S_y\right)\right]$$

$$S_y\ \frac{dS_y}{dx}=2\left(\frac{2}{\pi}\right)^{0.5}W_{eff}\ \ \frac{d\sigma_{ya}}{dx}\left[x=\sigma_{ya}{}^{-1}\left(\left(\frac{2}{\pi}\right)^{0.5}W_{eff}\right)\right]$$

The above logic ensures that $W_{eff}$ increases more slowly than $S_y$, ensuring that b will reduce to zero and the HEGADAS concentration profile reduces to a Gaussian profile[2].

3. *Pure passive dispersion (b=0)*

   After b has reduced to zero, the passive-dispersion crosswind concentration profile is imposed. The entrainment equation, and the equation defining the growth of Gaussian profile are given by

$$\frac{d}{dx}\left[\frac{H_{eff}u_{eff}}{V_m}\right]=\frac{u_{top}(u_T)}{V_0}+Q_{wv}\ ,\quad u_e(u_T)=\frac{\kappa\, u_T}{\Phi(Ri_*(u_T)}$$

$$S_y=2^{1/2}\sigma_{ya}(x+x_v)$$

   where $x_v$ is the virtual distance chosen such that $S_y$ is continuous at the transition point $x_t$ at which b reduces to zero.

### 4.5.3 Gravity-spreading formulation for future implementation

The proposed UDM model for future implementation may assume that the dense gas cloud passes through three consecutive stages of lateral cloud growth:

*1. Gravity spreading*.

The adopted equations are identical to those of the current UDM version prior to the passive transition, i.e.

$$\frac{dm_{cld}}{ds}=\frac{d}{ds}\left[2W_{eff}H_{eff}(1+h_d)u_{cld}\rho_{cld}\right]\ =\ \left[2W_{eff}u_{top}+\ H_{eff}(1+h_d)u_{side}\right]\rho_a+\frac{dm_{wvg}}{ds}\ ,\quad u_{side}=\gamma\frac{dW_{eff}}{dt},\ u_{top}=\frac{\kappa\, u_*}{\Phi(Ri_*)}$$

$$\frac{dW_{eff}}{dt}=C_E\ u_*\ \sqrt{Ri_*}$$

The above logic applies as long as the HEGADAS 'gravity current collapse criterion' (3) is not satisfied.

*2. Post-collapse gravity spreading (before or at passive transition??), and passive dispersion*

After the above criterion is satisfied, a reduced gravity-spreading rate needs to be applied, and in line with HEGADAS a modified entrainment equation. The HEGADAS logic can not be directly be translated to UDM logic. A better assumption may be to apply passive dispersion after collapse [including possible phasing in of passive dispersion along a transition].

This should only be done if the (phased-in) passive spread rate at this point would give a reduced spread rate. This would ensure that $W_{eff}$ increases more slowly.

Thus downwind of the point at which the above criterion is satisfied, the equations are as follows

$$\frac{dm_{cld}}{ds}=\frac{d}{ds}\left[2W_{eff}H_{eff}(1+h_d)u_{cld}\rho_{cld}\right]\ =\ 2\,W_{eff}\left[\frac{1}{\sigma_y}\frac{d\sigma_{ya}}{dx}+\frac{1}{\sigma_z}\frac{d\sigma_{za}}{dx}\right]u_a(z=z_c)\ \rho_a(z=z_c)+\frac{dm_{wv}{}^{gnd}}{ds}$$

$$\frac{d\sigma_y}{dx}=\frac{d\sigma_{ya}}{dx}$$

[2] TO CHECK: The right-hand side for the differential equation for $S_y$ is to be further checked.

Note that passive dispersion is phased in along a transition zone.

## 4.6 Validation against HTAG experiments

### 4.6.1 Selection of experiments

The following experiments could be considered for validating the gravity-spreading formulation:

1. The HTAG wind tunnel experiments have been extensively analysed by Roberts [see Chapter 8 in HGSYSTEM 1.0 Technical Reference Manual; see Section 8.3.1 for HEGADAS input)] to study crosswind spreading. HTAG experiments 86-91 involve point sources with significant jet entrainment and are less appropriate. HTAG experiments 139 and 140 (from a ground-level area source) seem to be most appropriate. They consider isothermal dispersion of a heavy ideal gas from a ground-level circular area source. UDM modelling complexities include the modelling of the circular area source and imposing appropriate passive dispersion coefficients (the UDM profiles for atmospheric dispersion coefficients cannot be applied to wind tunnels).

2. The large-scale Maplin Sand Experiments do not involve the problem with the application of passive dispersion, but again involves the additional complexity of appropriate modelling of the evaporating propane pool. Including the pool evaporation/spreading modelling would not allow us to concentration on the crosswind-spreading formulation only (additional inaccuracies may result from the pool model predictions). Also the appropriate pool segment needs to be selected.

3. Alternatively, the additional experiments described in the paper by Roberts and Hall[xii] may be considered.

4. The HF Goldfish runs involve complexity of HF thermodynamics. The correct implementation of the thermodynamics should be investigated first, before proceeding in investigating the width and cross-wind profiles.

5. If comparison against a specific experiment gives a problem, a specific AEROPLUME/HEGADAS run could be carried out (not involving pool calculations and involving heavy dispersion; but this may be hard to obtain)

As a result of the above the HTAG experiments 139 and 140 have been selected for initial further investigation.

### 4.1.2 Experimental parameters and experimental results

The HTAG experiments 139 and 140 are characterised as follows:

1. ambient data:

   * pressure = 0.85 atmosphere, temperature = 20C
   * surface roughness = 0.015 m, speed 5.6 m/s at 10 m height
   * passive cross-wind dispersion coefficient $\sigma_{ya}(x) = 0.63\ x^{0.6}$ [$d\sigma_{ya}/dx=0.378x^{-0.4}$]; vertical dispersion coefficient $\sigma_{za}(x)$= ??? [this may be derived from experimental data]
   * relative humidity = 0% (assumed value)

2. pollutant properties [HT139 (gas/air density ratio = 1.4) and HT140 (gas air/density ratio 3.9)]. These are to be simulated by adjusting molecular weight of air [new components named GAS_HT139 and GAS_HT140). Using the air molecular weight $M_a$ = 28.96 kg/kmole and the air density $\rho_a$ = 0.85*1.204 kg/m$^3$, this implies:

   - HT139: $M_{pol} = 1.4*M_a$ = 40.5 kg/kmole, $\rho_{pol} = 1.4*\rho_a$ =0.85*1.686 kg/m$^3$
   - HT140: $M_{pol} = 3.9*M_a$ = 113 kg/kmole, $\rho_{pol} = 3.9*\rho_a$ =0.85*4.696 kg/m$^3$

3. isothermal conditions (air, ground and gas all 20C); no heat and water-vapour transfer

4. release data:
   * circular ground-level source with diameter of 5.08 m [area = 20.25 m$^2$, equivalent HEGADAS square pool length = 4.5 m]
   * volume flow rate = 22 m$^3$/s[3]. Thus the release rates are:

     - HT139: Q = 22 $\rho_{pol}$ = 22*0.85*1.686 = 31.5 kg/s
     - HT140: Q = 22 $\rho_{pol}$ = 22*0.85*4.696 = 87.8 kg/s

[3] HEGADAS adopts 1 atm. ambient pressure; this leads to 15% reduced volume flow rate of 0.85*22=18.7 m$^3$/s, and 15% increased air/pollutant densities. The value for the release rate Q is the same.

See Chapter 8 in the HGSYSTEM 1.0 Technical Reference Manual for the experimental data.

### 4.6.2 UDM and HEGADAS predictions

UDM simulations have been carried out, and results have been compared with the experimental data and HEGADAS simulations.

HEGADAS simulations
Three type of HEGADAS simulations were carried out, i.e.:

(a) Simulation using experimentally observed value $\sigma_{ya} = 0.63\ x^{0.6}$ of cross-wind dispersion coefficient $\sigma_{ya}$, and calculations including gravity-spreading collapse

(b) Simulation using standard atmospheric value of cross-wind dispersion coefficient $\sigma_{ya}$, and calculations including gravity-spreading collapse

(c) Simulation using standard atmospheric value of cross-wind dispersion coefficient $\sigma_{ya}$, and calculations excluding gravity-spreading collapse ($C_D$=0 as HEGADAS input)

The HEGADAS power-law fit $u(z) = [u_o/z_o]^p$ results in the exponent value p = 0.23. The HEGADAS vertical concentration profile adopts an exponent n = 1+p = 1.23. The release from the ground-level pool results in the formation of a 100% gas blanket.

UDM simulations

The following is applied.

1. Two types of power-law fits to the ambient wind speed profile are applied:
   * The standard UDM power-law fit $u(z) = [u_{ref}/z_{ref}]^p$ fit to the ambient wind speed profile resulting into the exponent value p = 0.14
   * the HEGADAS value p = 0.23

2. Two types of vertical concentration profile
   * The standard assumption of Gaussian vertical concentration profile (n=2; automatically applied by selecting stability class D)
   * the HEGADAS value n = 1.23

3. UDM can strictly speaking only deal with a jet release and not with a release from a ground-level pool. Modelling a ground-level pool as a vertical jet would not be accurate. As a result, HEGADAS values are imposed at the downwind edge of the HEGADAS gas blanket. The data needed for this initialisation are: downwind distance of downwind edge of gas blanket $x_{bl}$, zero plume height, maximum concentration $c_{ov}$, cloud half-width $W_{eff}$. To this purpose a special UDM version was generated to enable to hardwire the downwind distance $x_{bl}$ and the cloud half-width $R_y$.

4. The UDM atmospheric profiles for the passive dispersion coefficients $\sigma_{ya}$ and $\sigma_{za}$ are applied, although it is recognised that this may lead to inaccurate passive-dispersion predictions [alternative and more preferable would be to overwrite default values for $\sigma_{ya}$, $d\sigma_{ya}/dx$ to impose $\sigma_{ya} = 0.63\ x^{0.6}$, and similar to $\sigma_{za}$; however this requires for us to establish the value for $\sigma_z$]

5. The value of the collapse gravity criterion is monitored, to establish where gravity collapse may occur.

Results

Figure 4.7 and Figure 4.8 include UDM/HEGADAS results for experiments HT139 and HT140, respectively. Results are included for the effective cloud half-width $B_{eff}$, the SMEDIS cloud half-width b, and the centre-line ground-level concentration $c_{ov.}$ The UDM assumptions for the wind speed power-law fit and the vertical concentration profile are chosen to be in line with the HEGADAS assumptions (p = 0.2, n = 1.2). The following conclusions can be drawn:

1. The UDM results are in close agreement with the results of the HEGADAS simulation (no gravity collapse, standard $\sigma_{ya}$):
   * Results for effective cloud half-width (Figure 4.7a and Figure 4.8a) and centre-line concentration (Figure 4.7c and Figure 4.8c) are virtually identical

* The UDM predictions for the SMEDIS cloud half-width are larger than the HEGADAS results (Figure 4.7b and Figure 4.8b). This is the result of the difference in the shape of the cross-wind concentration profiles. HEGADAS adopts a profile with a middle part of uniform concentration and outer flanks with Gaussian decay.

2. The HEGADAS simulation (gravity collapse, standard $\sigma_{ya}$) demonstrates that inclusion of gravity-spreading collapse significantly reduces the cloud half-widths and increases the centre-line ground-level concentration.

3. The HEGADAS simulation (gravity collapse, experimental $\sigma_{ya}$) demonstrates that the experimental $\sigma_{ya}$ (lower than the standard atmospheric $\sigma_{ya}$) leads to further reduced cloud half-widths and larger concentrations.

Figure 4.9 and Figure 4.10 include results of HEGADAS (standard $\sigma_{ya}$, no gravity collapse, p = 0.2, n = 1.2), UDM with HEGADAS assumptions (standard $\sigma_{ya}$, no gravity collapse, p = 0.2, n = 1.2), and the standard UDM model (standard $\sigma_{ya}$, no gravity collapse, p =0.14, s = 2). For the UDM centroid height less than the reference height $z_{ref}$ = 10 m, the larger s value results in the larger wind-speed and consequently somewhat smaller cloud half-widths and larger centre-line ground-level concentrations.

Figure 4.11 includes crosswind concentration profiles at a range of downwind distances (compare plots in Chapter 8 of HGSYSTEM 1.0 Technical Reference Manual). It demonstrates the development from a top-hat profile in the near-field (with large cloud densities) into a Gaussian profile (with cloud density close to ambient density).

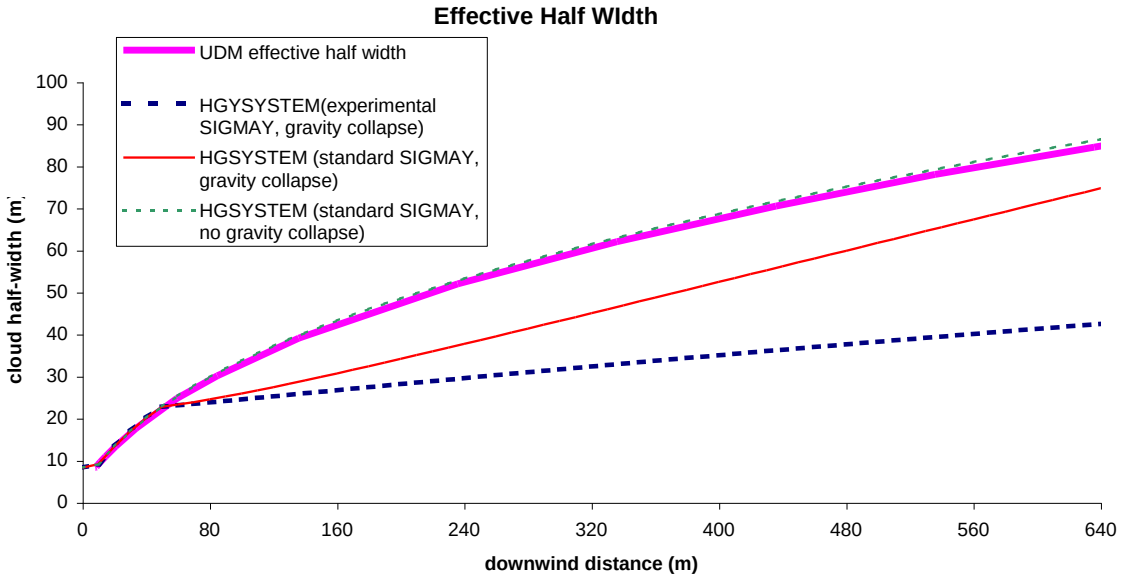


**Figure 4.7 (a) effective cloud half-width $W_{eff}$**

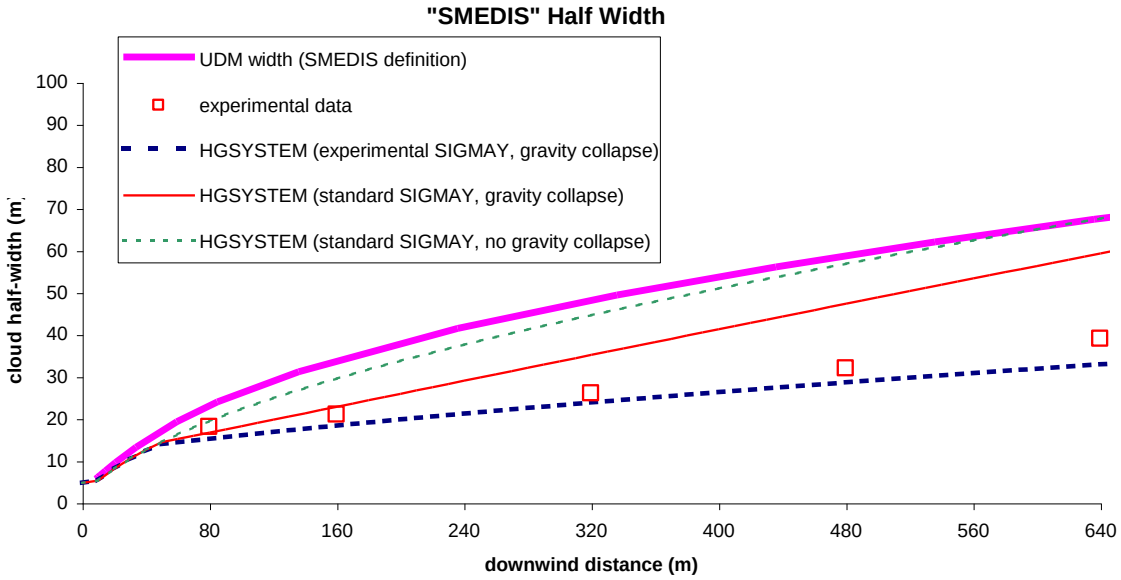


**Figure 4.7 (b) cloud half-width (SMEDIS definition)**

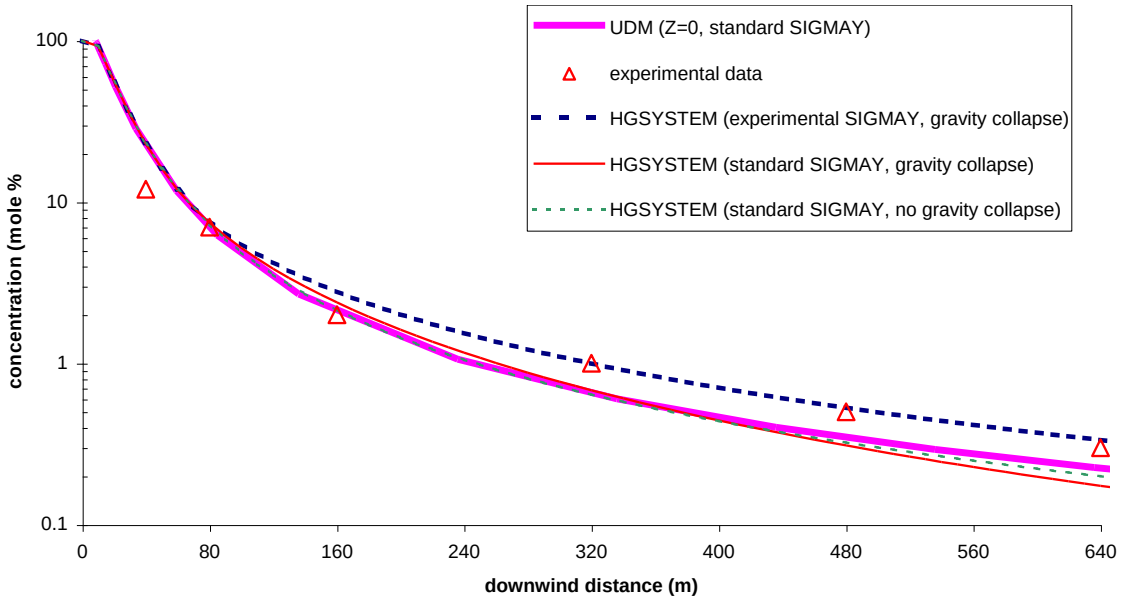


**(c) centre-line ground-level concentration**

**Figure 4.7.** **UDM and HEGADAS simulations for HT139 (p = 0.2, n = 1.2); curves included are as follows:**

- **experimental data**
- **HEGADAS (experimental $\sigma_{ya}$ , gravity collapse)**
- **HEGADAS (standard $\sigma_{ya}$ , gravity collapse)**
- **HEGADAS (standard $\sigma_{ya}$ , no gravity collapse)**
- **UDM 6.0 (standard $\sigma_{ya}$ , no gravity collapse)**

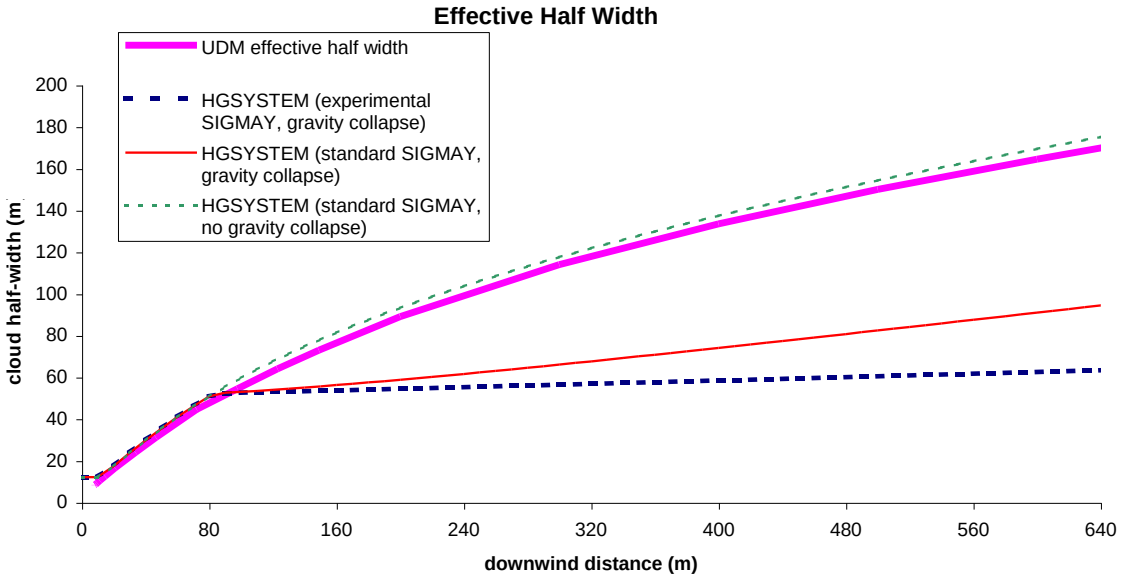


**Figure 4.8 (a) effective cloud half-width $W_{eff}$**

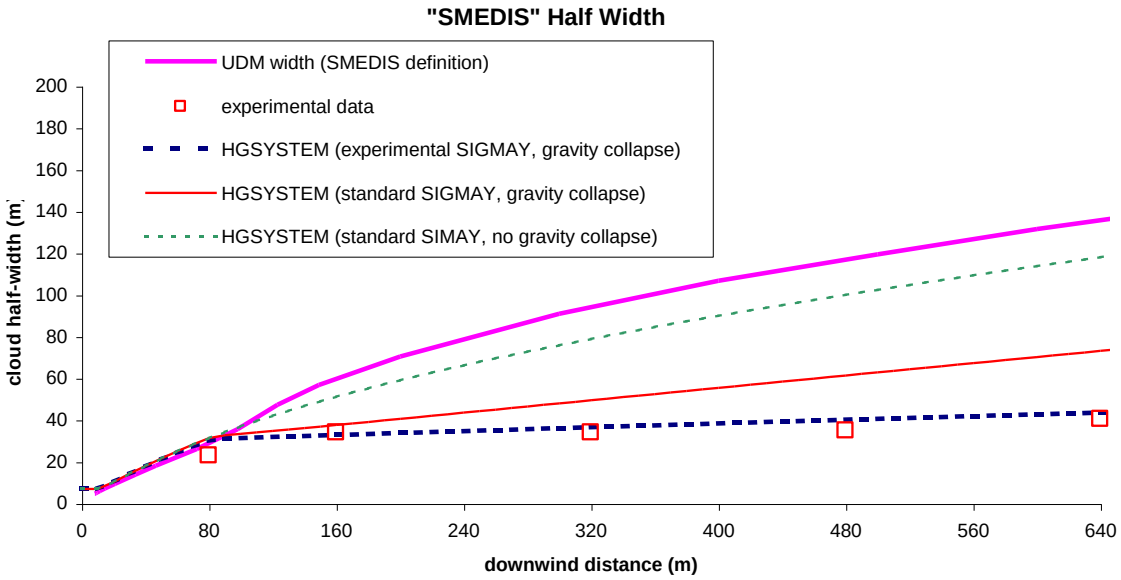


**Figure 4.8 (b) cloud half-width (SMEDIS definition)**

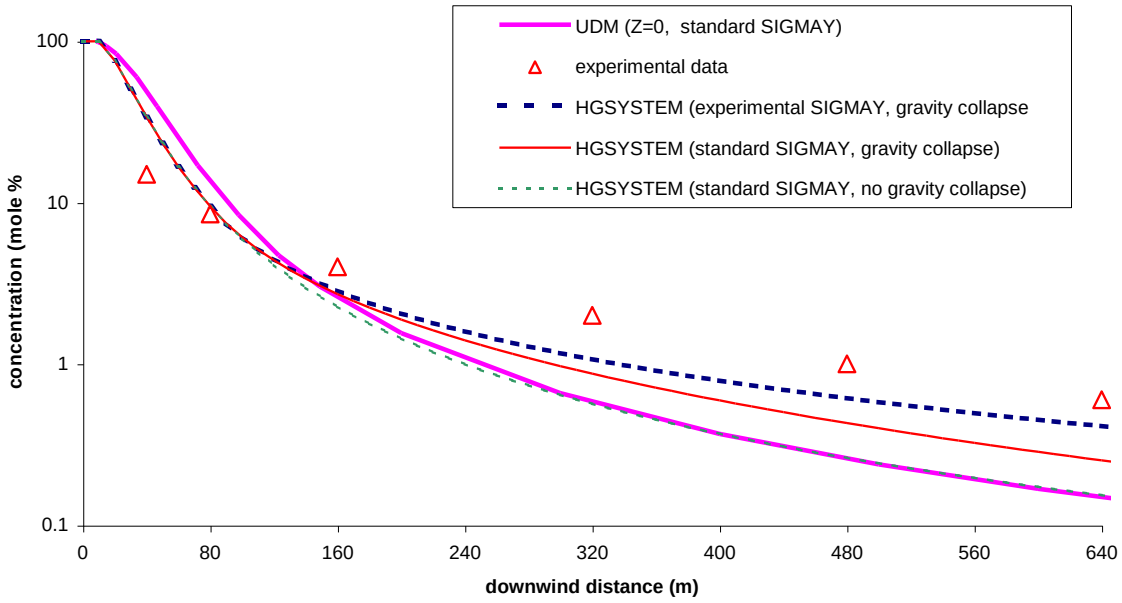


**(c) centre-line ground-level concentration**

**Figure 4.8.** **UDM and HEGADAS simulations for HT140 (p = 0.2, n = 1.2); curves included are as follows:**

- **experimental data**
- **HEGADAS (experimental $\sigma_{ya}$ , gravity collapse)**
- **HEGADAS (standard $\sigma_{ya}$ , gravity collapse)**
- **HEGADAS (standard $\sigma_{ya}$ , no gravity collapse)**
- **UDM 6.0 (standard $\sigma_{ya}$ , no gravity collapse)**

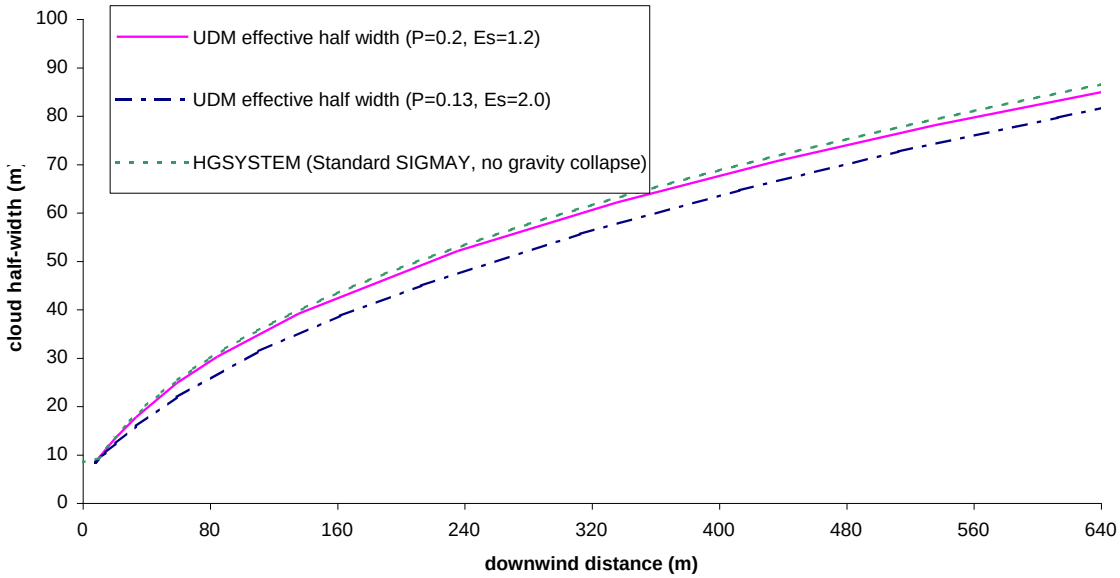


**(a) cloud effective half-width**

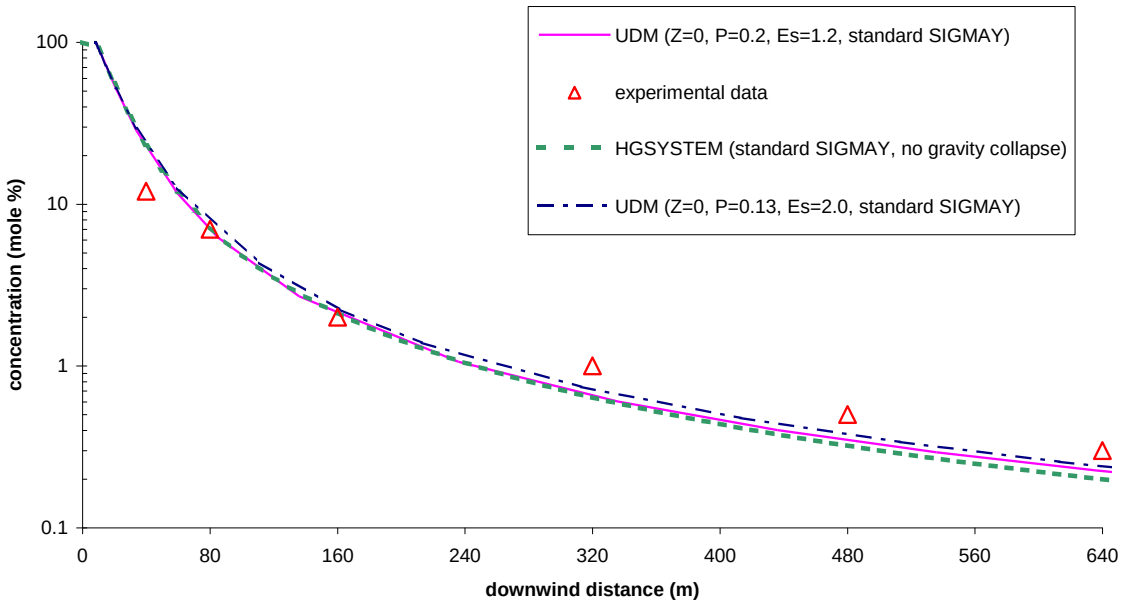


**(b) centre-line concentration**

**Figure 4.9.** **UDM and HEGADAS simulations for HT139; curves included are as follows:**

- **experimental data**
- **HEGADAS (standard $\sigma_{ya}$ , no gravity collapse; p=0.2,n=1.2)**
- **UDM 6.0 (standard $\sigma_{ya}$ , no gravity collapse; p=0.2,n=1.2)**
- **UDM 6.0 (standard $\sigma_{ya}$ , no gravity collapse; p=0.13,n=2)**

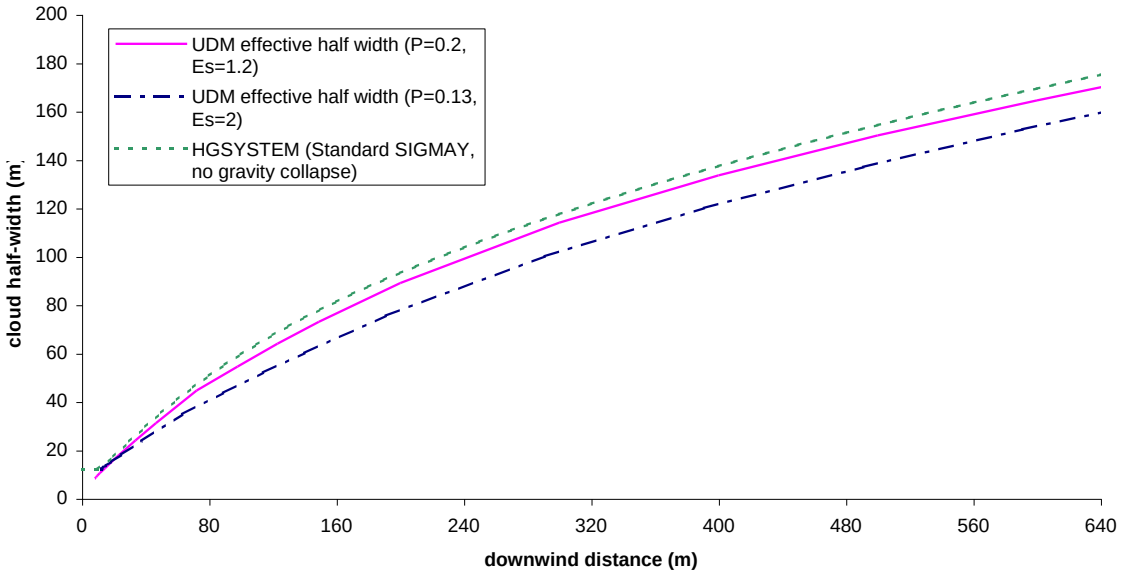


**(a) cloud effective half-width**

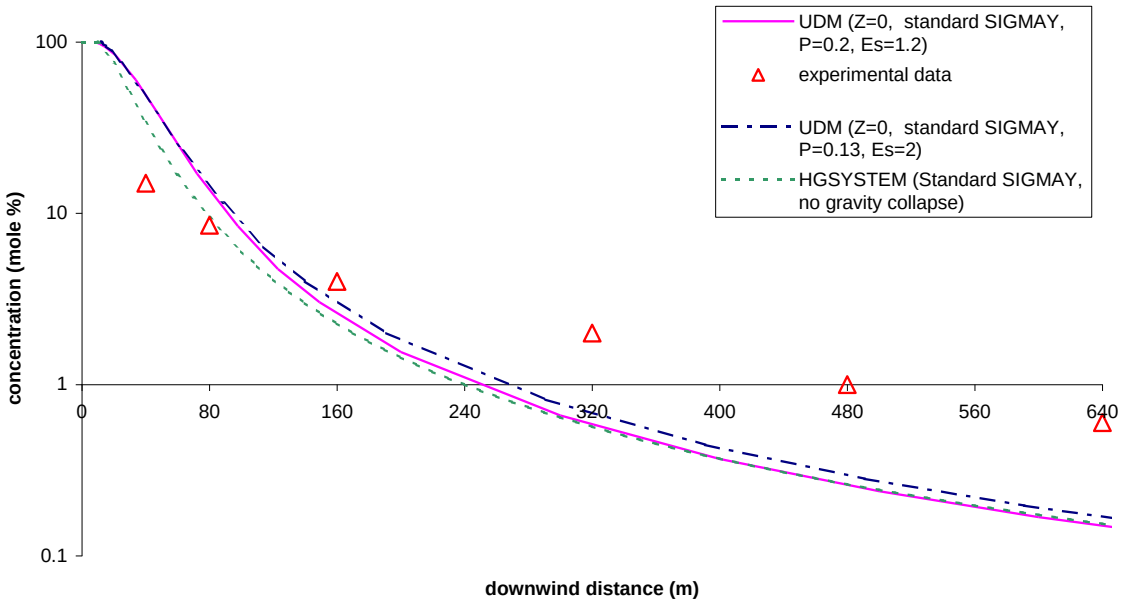


**(b) centre-line concentration**

**Figure 4.10.** **UDM and HEGADAS simulations for HT140; curves included are as follows:**

- **experimental data**
- **HEGADAS (standard $\sigma_{ya}$ , no gravity collapse; p=0.2,n=1.2)**
- **UDM 6.0 (standard $\sigma_{ya}$ , no gravity collapse; p=0.2,n=1.2)**
- **UDM 6.0 (standard $\sigma_{ya}$ , no gravity collapse; p=0.13,n=2)**

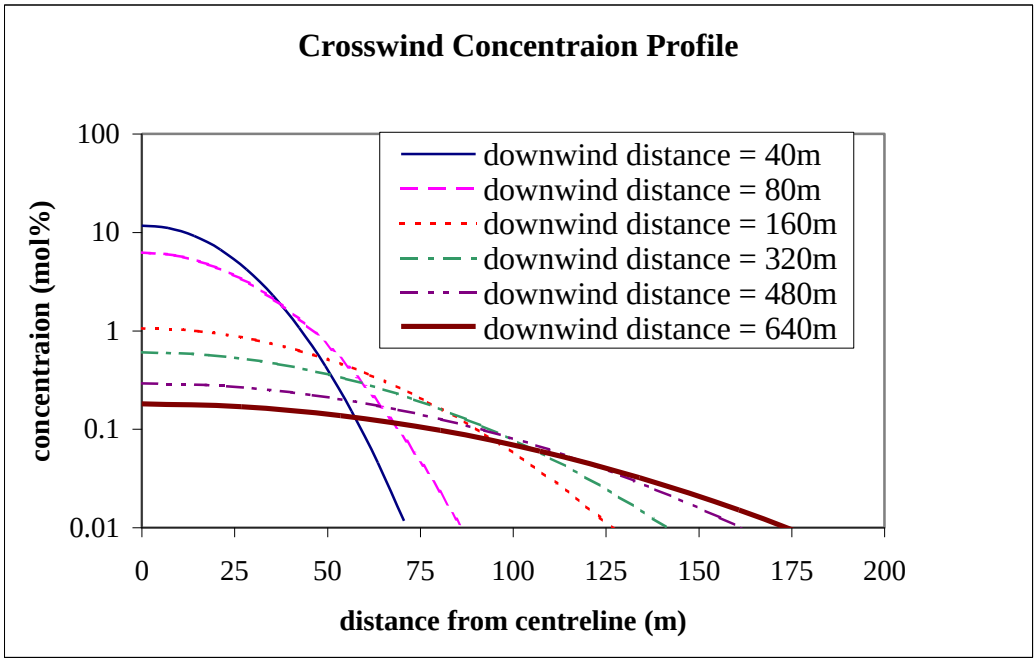


**(a) HT139**

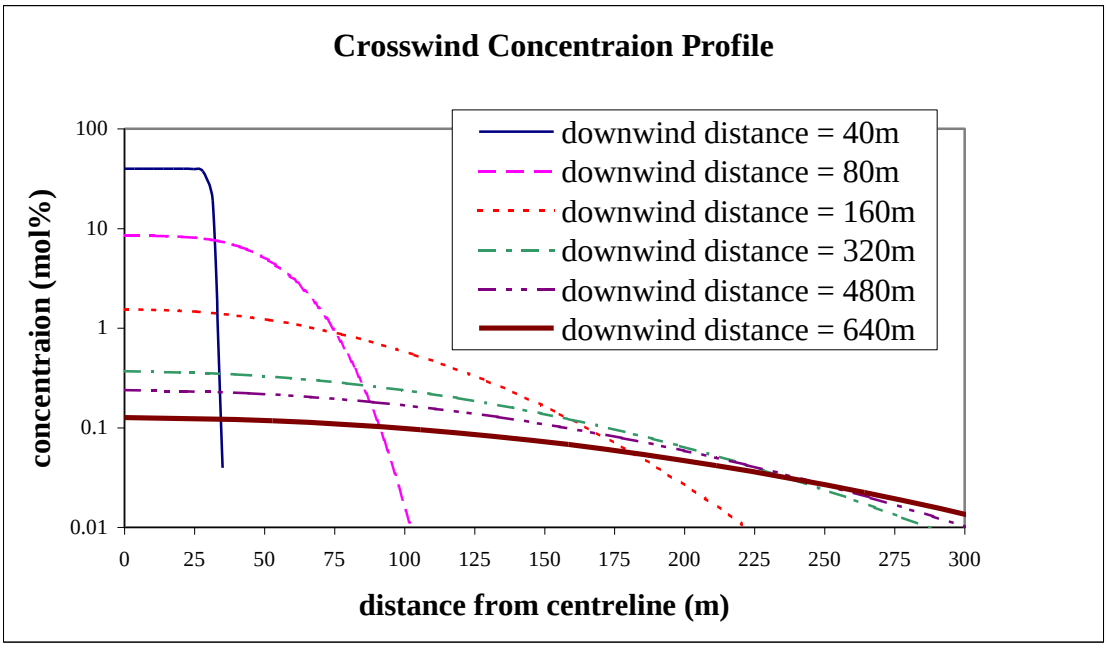


**(b) HT140**

**Figure 4.11. UDM predictions (p=2, n=1.2) of cross-wind concentration profiles (HT139, HT140)**

## 4.7 Further work

1. Inclusion of the collapse of gravity spreading is recommended into the gravity-spreading formulation, in line with the HGSYSTEM formulation[v]. Subsequent validation against the Maplin Sand experiments, HTAG wind-tunnel experiments, and further experiments by Roberts and Hall[xii].

2. A sensitivity analysis is to be carried out for a given base-case problem, with a selected number of single/multiple parameter variations.

3. Possible modification of the calculation of the friction velocity for non-isothermal problems (in line with HEGADAS logic; $u_T$ instead of $u_*$).

Further study of the TUV experiments, to check for possible stability-class dependency of the top-entrainment formulation.

## SPREADSHEETS

| | |
|---|---|
| Figure 4.1 | ENTFUN.xls |
| Figure 4.2 | McQd2Ana.xls |
| Figure 4.3 | McQuaid3+Jet.xls |
| Figure 4.4 | McQuaid1+Jet.xls |
| Figure 4.5 | McQuaid2+Jet.xls |
| Figure 4.6 | McQuaid3+Jet.xls |
| Figure 4.7 | HTG139HG.xls |
| Figure 4.8 | HTG140HG.xls |
| Figure 4.9 | HT139UMP.xls |
| Figure 4.10 | HT140UMP.xls |
| Figure 4.11a | HTG139HG.xls |
| Figure 4.11b | HTG140HG.xls |

## About DNV

We are the independent expert in risk management and quality assurance. Driven by our purpose, to safeguard life, property and the environment, we empower our customers and their stakeholders with facts and reliable insights so that critical decisions can be made with confidence. As a trusted voice for many of the world's most successful organizations, we use our knowledge to advance safety and performance, set industry benchmarks, and inspire and invent solutions to tackle global transformations.

## Digital Solutions

DNV is a world-leading provider of digital solutions and software applications with focus on the energy, maritime and healthcare markets. Our solutions are used worldwide to manage risk and performance for wind turbines, electric grids, pipelines, processing plants, offshore structures, ships, and more. Supported by our domain knowledge and Veracity assurance platform, we enable companies to digitize and manage business critical activities in a sustainable, cost-efficient, safe and secure way.

DNV | digital@dnv.com | dnv.com/digital

# REFERENCES


[i] "Guidelines for use of vapour cloud dispersion models", Second Edition, CCPS, New York (1996)

[ii] Lees, F.P., "Loss Prevention in the process industries – hazard identification, assessment and control", Butterworth-Heineman, Oxford, UK (1994)

[iii] Witlox, H.W.M, "Technical description of the heavy-gas dispersion program HEGADAS", Shell External Report TNER.93.0032, Thornton Research Centre (1993)

[iv] McFarlane, K., Prothero, A., Puttock, J.S., Roberts, P.T., and Witlox, H.W.M., "Development and validation of atmospheric dispersion models for ideal gases and hydrogen fluoride", Part I: Technical Reference Manual, Shell Report TNER.90.015, Thornton Research Centre (1990)

[v] Post. L. (editor), "HGSYSTEM 3.0 Technical Reference Manual". Shell External Report TNER.94.059, Thornton Research Centre (1994)

[vi] Witlox, H.W.M., "Evaluation of the dense gas dispersion program HEGADAS against 2-D wind tunnel experiments", Shell Report TNGR.89.108, Thornton Research Centre (1989)

[vii] Havens, J., and Spicer, T.O.,"Development of an atmospheric dispersion model for heavier-than-air mixtures" (DEGADAS mode), Vols. 1- 3, University of Arkansas (1985)

[viii] Britter, R.E., "A review of mixing experiments relevant to dense gas dispersion", IMA Conference on stably stratified flow and dense gas dispersion ", April 1986, Chester, Oxford University Press (1988)

[ix] McQuaid, J., "Some experiments on the structure of stably stratified shear flows", Technical Paper P21, Safety in Mines Research Establishment, Sheffield, UK (1976)

[x] Witlox, H.W.M., Mathematical modelling of three-dimensional dense-gas-dispersion problems, in "Waves and turbulence in stably stratified flows" (Mobbs, S.D. and King, J.C., eds.), pp. 363-394, Clarendon Press, Oxford (1993)

[xi] Van Ulden, A.P., "A new bulk model for dense gas dispersion: two-dimensional spread in still air, in "Atmospheric dispersion of heavy gases and small particles" (Ooms, G. and Tennekes, H., eds.), pp. 419-440, Springer-Verlag, Berlin (1984)

[xii] Roberts, P.T., and Hall, D.J., "Wind tunnel simulation. Boundary layer effects in dense gas dispersion experiments", J. Loss Prevention Process Ind. 7 (1994)